Short Communication

Synthesis and characterization of *trans*-phenylethynylalkynyl adducts on a tetraanilinopyridinato-diruthenium(III) core

Guolin Xu, Tong Ren *

*Department of Chemistry and Center for Supramolecular Science, University of Miami, P.O. Box 249118 Coral Gables, FL 33124-0431, USA*

Abstract

Treating $Ru_2(ap)_4Cl$ with large excess of LiC_2Ph led to the isolation of previously unidentified *trans*-$Ru_2(ap)_4(C_2Ph)_2$ (**2a**) where *ap* is 2-anilinopyridinate. Reactions between $Ru_2(ap)_4(C_2X)$ and LiC_2Ph in excess yielded similar bis-alkynyl compounds *trans*-$(PhC_2)[Ru_2(ap)_4](C_2X)$ (X = $SiMe_3$, **2b**, C_2SiMe_3, **2c**). Also reported are electrochemical and spectroscopic characterizations of compounds **2a–c** and X-ray structural analysis of compounds **2a** and **2b**. © 2002 Elsevier Science B.V. All rights reserved.

Keywords: Bis-alkynyl compounds; *trans*-phenylethynylalkynyl adducts; Tetraanilinopyridinato-diruthenium(III) core

1. Introduction

Isolation of $Ru_2(ap)_4(C_2Ph)$ (**1a** in Scheme 1, *ap* = 2-anilinopyridinate) by Chakravarty and Cotton in 1986 marked the first example of paddlewheel species bearing an alkynyl ligand [1]. Subsequently, many examples of diruthenium complexes bearing axial alkynyl ligands have been reported by the laboratories of Bear [2–4] and Ren [5–12]. In the original work of Chakravarty and Cotton, treating $Ru_2(ap)_4Cl$ with five equivalent of LiC_2Ph produced **1a** as the only product in 70% yield [1]. On the other hand, treating $Ru_2(F_5ap)_4Cl$ (F_5ap is 2-pentafluoroanilinopyridinate) with 50 equivalent of LiC_2Ph led to the isolation of both the expected $Ru_2(F_5ap)_4(C_2Ph)$ and *trans*-$[Ru_2(F_5ap)_4](C_2Ph)_2$, a bis-phenylethynyl adduct [4]. Recently, we found that the bis-alkynyl adducts of the $Ru_2(ap)_4$ core can also be synthesized with either butadiynyl [9] or butadiynyl/ethynyl ligands [11]. Naturally, one would wonder if the bis-phenylethynyl adduct on a $Ru_2(ap)_4$ core could be isolated by using a large excess of LiC_2Ph. Reported herein are the isolation and structural characterization of the previously unidentified bis-adduct (**2a**, Scheme 1).

In addition, we also synthesized and characterized the mixed alkynyl bis-adducts (**2b** and **2c**).
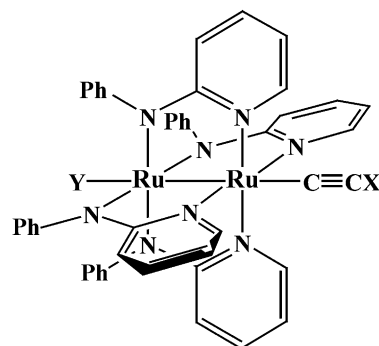
1, X = Ph (**1a**), $SiMe_3$ (**1b**), C_2SiMe_3 (**1c**); Y = none
2, X = Ph (**2a**), $SiMe_3$ (**2b**), C_2SiMe_3 (**2c**); Y = C_2Ph

Scheme 1. Mono-(**1**) and bis-alkynyl (**2**) adducts of $[Ru_2(ap)_4]$ core.

2. Results and discussion

When $Ru_2(ap)_4Cl$ was treated with five equivalents of LiC_2Ph, the solution became brown, and the mono-phenylacetylide adduct (**1a**) was the only isolated product [1]. When the quantity of LiC_2Ph was increased to 20 equivalents in the present study, the reaction mixture turned immediately to dark red, a color that was attributed to the formation of

* Corresponding author. Tel.: +1-305-2846617; fax: +1-305-2841880
E-mail address: tren@miami.edu (T. Ren).

$\{RC_2[Ru_2(ap)_4]C_2R'\}^{1-}$ in an earlier study [11]. Subsequent workup resulted in the isolation of *trans*-$[Ru_2(ap)_4](C_2Ph)_2$ (**2a**, 72%) in addition to a small quantity of **1a**. Clearly, an equilibrium between the mono-adduct (**1**) and $\{RC_2[Ru_2(ap)_4]C_2R'\}^{1-}$ exists in solution when excess LiC_2R is used [11]. A large excess of lithiated alkynyl drives the equilibrium towards the bis-adduct formation. Similarly, treating $[Ru_2(ap)_4]C_2X$ (X = $SiMe_3$, **1b** and C_2SiMe_3, **1c**) with 30 equivalents of LiC_2Ph yielded the dissymmetric bis-adducts *trans*-$(PhC_2)[Ru_2(ap)_4](C_2X)$ (**2b/2c**). It was noted previously that $[Ru_2(ap)_4](C_2SiMe_3)$ was the sole product when $Ru_2(ap)_4Cl$ was treated with 10-fold LiC_2SiMe_3 [9]. Facile formation of **2** reveals that the subtle difference in steric bulkiness between Me_3Si and Ph groups differentiates their abilities in coordinating to the Ru center flanked by the anilino groups. Similar to the previously studied bis-alkynyl adducts, compounds **2a**–**2c** are diamagnetic, which facilitate their characterization using both ^1H- and ^{13}C-NMR spectroscopic techniques.

Both compounds **2a** and **2b** were crystallized successfully and their structures, shown respectively in Figs. 1 and 2, were determined via single crystal X-ray diffraction studies. Some key bond lengths and angles of both **2a** and **2b** are gathered in Table 1. Clearly, the *ap* ligands in both **2a** and **2b** adopt the (4,0) arrangement that is common among the alkynyl adducts on a $Ru_2(ap)_4$ core [1,7,9,11]. The Ru–Ru bond lengths are 2.4707(3) and 2.4342(8) Å in molecules **2a** and **2b**, respectively, and comparable to that observed for other $RC_2[Ru_2(ap)_4]C_2R'$ compounds (2.458–2.472 Å) [9,11]. Compared with the respective mono-alkynyl molecules **1a** [1] and **1b** [7], the Ru–Ru bond lengths have been increased by 0.162 Å in **2a** and 0.128 Å in **2b**. The significant lengthening of Ru–Ru bond is clearly attributed to the formation of strong σ(Ru–C) bonds (1.988 [2] Å in **2a** and 1.966 [7] Å in **2b**) at the expense of σ(Ru–Ru) bond.

Structural studies of $Ru_2L_4(C_2R)_2$ type compounds revealed that the first coordination sphere of Ru_2 core deviates significantly from the idealized D_{4h} geometry [3–5,9–11], and the observed distortion was attributed
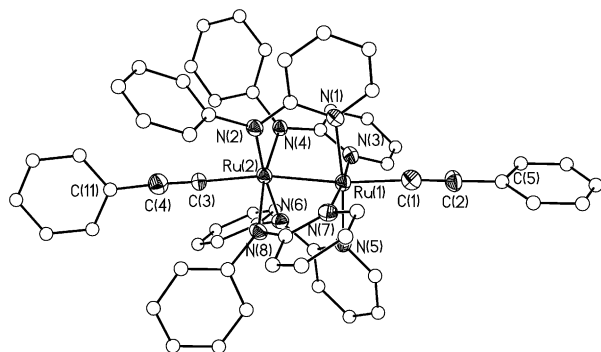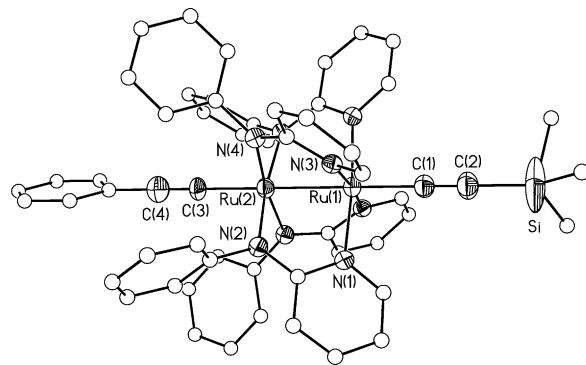

Fig. 2. ORTEP plot of molecule **2b** at 30% probability level.

Table 1
Selected bond lengths (Å) and angles (°) for compounds **2a** and **2b**

2a		2b	
Bond lengths			
Ru(1)–Ru(2)	2.4707(3)	Ru(1)–Ru(2)	2.4342(8)
Ru(1)–N(1)	2.065(2)	Ru(2)–N(2)	2.056(4)
Ru(1)–N(3)	2.153(2)	Ru(2)–N(4)	2.055(4)
Ru(1)–N(5)	2.051(2)	Ru(2)–C(3)	1.957(7)
Ru(1)–N(7)	2.000(2)	Ru(1)–N(1)	2.065(3)
Ru(2)–N(2)	2.029(2)	Ru(1)–N(3)	2.069(4)
Ru(2)–N(4)	1.988(2)	Ru(1)–C(1)	1.975(7)
Ru(2)–N(6)	2.024(2)	C(1)–C(2)	1.165(10)
Ru(2)–N(8)	2.183(2)	C(3)–C(4)	1.170(10)
Ru(1)–C(1)	1.987(2)		
C(1)–C(2)	1.205(3)		
Ru(2)–C(3)	1.989(2)		
C(3)–C(4)	1.203(3)		
Bond angles			
N(1)–Ru(1)–Ru(2)	86.67(5)	N(1)–Ru(1)–Ru(2)	87.16(9)
N(3)–Ru(1)–Ru(2)	78.35(5)	N(3)–Ru(1)–Ru(2)	86.67(10)
N(5)–Ru(1)–Ru(2)	87.09(5)	N(2)–Ru(2)–Ru(1)	86.31(10)
N(7)–Ru(1)–Ru(2)	96.08(5)	N(4)–Ru(2)–Ru(1)	86.04(10)
C(1)–Ru(1)–Ru(2)	164.24(8)	C(3)–Ru(2)–Ru(1)	180
C(2)–C(1)–Ru(1)	175.8(2)	C(1)–Ru(1)–Ru(2)	180
N(2)–Ru(2)–Ru(1)	86.35(5)		
N(4)–Ru(2)–Ru(1)	93.51(5)		
N(6)–Ru(2)–Ru(1)	86.40(5)		
N(8)–Ru(2)–Ru(1)	76.27(5)		
C(3)–Ru(2)–Ru(1)	161.74(7)		
C(4)–C(3)–Ru(2)	179.5(2)		

Fig. 1. ORTEP plot of molecule **2a** at 30% probability level.

to a second order Jahn–Teller effect [5]. The same distortion is present in **2a**, as reflected by the large discrepancy in Ru–N bond lengths. On the Ru(1) center, Ru(1)–N(3) bond length is 2.153(2) Å, while the bond *trans* to it, Ru(1)–N(7), is only 2.000(2) Å long. On the Ru(2) center, the length difference between the long (Ru(2)–N(8)) and short (Ru(2)–N(4)) bonds is 0.195 Å, the largest observed for $Ru_2L_4(C_2R)_2$ type compounds [12]. Concurrent with the elongation/compression of Ru–N bonds, Ru–Ru–C bond angles deviate from the linearity by at least 15°. In contrast, molecule **2b** has a crystallographic twofold axis containing both the Ru atoms and all acetylenic carbon atoms,

$$\{PhC_2[Ru_2]C_2R\}^+ \xrightleftharpoons[\mathbf{A}]{+\ e^-} PhC_2[Ru_2]C_2R \xrightleftharpoons[\mathbf{B}]{+\ e^-} \{PhC_2[Ru_2]C_2R\}^- \xrightleftharpoons[\mathbf{C}]{+\ e^-} \{PhC_2[Ru_2]C_2R\}^{2-}$$

$$\downarrow -(C_2Ph)^{1-}$$

$$[Ru_2]C_2R \xleftarrow[\mathbf{D}]{-\ e^-} \{[Ru_2]C_2R\}^-$$

Scheme 2. Assignment of redox couples and related chemical step.

which constrains both Ru–Ru–C bond angles to exactly 180°. In addition, lengths of Ru(1)–N(1) and Ru(1)–N(3), two independent Ru–N(py) bonds, are identical within the experimental errors. The same is also true about two independent Ru–N(anilino) bonds (Ru(2)–N(2) and Ru(2)–N(4)). Clearly, molecule **2b** is not subject to a second Jahn–Teller distortion.

Rich redox chemistry has been the hallmark of diruthenium alkynyl complexes [1–13], and the compounds reported here are no exception. As shown in Fig. 3, cyclic voltammograms of compounds **2a**–**c** feature three one-electron redox couples: an oxidation (**A**, $Ru_2^{7+/6+}$), and two reductions (**B**, $Ru_2^{6+/5+}$, and **C**, $Ru_2^{5+/4+}$). These couples are either quasi-reversible or reversible, as indicated by both the ΔE values and $i_{back}/i_{forward}$ ratio. Among three compounds studied, **2b** has the most cathodically shifted couples, while **2c** has the most anodically shifted couples. Hence, the electrochemical studies reveal an order of donor strength: $Me_3SiC_2- > PhC_2- > Me_3SiC_4-$.

For all compounds studied here, the backward sweep of cathodic scan also features a small but detectable wave (**D**) between **B** and **C** couples. Similar to the case of $RC_4[Ru_2(ap)_4]C_2R'$ [11], wave **D** is attributed to the oxidation of $\{[Ru_2(ap)_4]C_2R\}^{-1}$, which was generated in situ by the dissociation of $(PhC_2)^-$ from $\{PhC_2[Ru_2(ap)_4]C_2R\}^{2-}$, as illustrated in Scheme 2. Consistent with this scheme, both **2a** and **2b** display pronounced wave **D** while the $i_{backward}/i_{forward}$ ratio of

couple **C** is significantly smaller than unity. On the other hand, wave **D** is barely detectable in **2c**, while the $i_{backward}/i_{forward}$ ratio of couple **C** is 0.97. Further corroborating the mechanism, $E_{pa}(\mathbf{D})$ of **2b** (-0.843 V) and **2c** (-0.713 V) are comparable to the $E_{1/2}(0/1-)$ observed for $Ru_2(ap)_4(C_2Si^iPr_3)$ (-0.877 V) [11] and $Ru_2(ap)_4(C_4SiMe_3)$ (-0.742 V) [9], respectively.

While the monoalkynyl compounds **1** exhibit two peaks (ca. 470 and 750 nm) in their absorption spectra [7,9], the bis-alkynyl compounds **2** exhibit four absorption maxima in visible-near infrared window (Fig. 4). Peaks observed at ca. 640, 480 and 440 nm, are tentatively assigned as $\pi(CCR)$ to $\pi^*/\delta^*(Ru_2)$ transitions. The intense charge-transfer band appear around 1030 nm is likely related to the $\pi(Ru-N)$ to π^*/δ^* (Ru_2) charge transfer [11]. The HOMO–LUMO gap (E_{op}) corresponding to this λ_{max} is about 1.20 eV. Furthermore, the HOMO–LUMO gap of the solvated species can also be calculated from electrode potentials:

$$E_{LUMO} - E_{HOMO} = e\{E_{1/2}(\mathbf{A}) - E_{1/2}(\mathbf{B})\}$$

and the calculated values are 1.14, 1.18 and 1.15 eV for compounds **2a**, **2b** and **2c**, respectively. Hence, a small HOMO–LUMO gap for **2** has been independently confirmed by both the optical and electrochemical techniques.

Fig. 3. Cyclic voltammograms of compounds **2a**–**c** recorded in 0.20 M THF solution of Bu_4NPF_6 at a scan rate of 0.10 V s^{-1}.

Fig. 4. Vis–NIR absorption spectra of compounds **2a**–**c** recorded in THF.

3. Conclusions

Three new bis-alkynyl adducts on the $Ru_2(ap)_4$ core have been synthesized and characterized. These results complement our earlier studies of $[Ru_2L_4](C_2R)_2$ type compounds. Especially noteworthy are compounds **2b** and **2c**, which, upon desilylation, can be converted to mono-functional synthons in the context of *Glaser* type coupling chemistry [14].

4. Experimental

Phenylacetylene and ^nBuLi were purchased from Aldrich, and silica gel from Merck. $Ru_2(ap)_4Cl$ [7], $Ru_2(ap)_4(C_2SiMe_3)$ [7] and $Ru_2(ap)_4(C_4SiMe_3)$ [9] were prepared as previously described. THF was distilled over Na–benzophenone under an N_2 atmosphere prior to use. ^1H- and ^{13}C-NMR spectra were recorded on a Bruker AVANCE300 NMR spectrometer, with chemical shifts (δ) referenced to the residual $CHCl_3$ and the solvent $CDCl_3$, respectively. Infrared spectra were recorded on a Perkin–Elmer 2000 FT-IR spectrometer using KBr disks. UV–vis spectra were obtained using a Perkin–Elmer Lambda-900 UV–Vis–NIR spectrophotometer. Cyclic voltammograms were recorded in 0.2 M ($^nBu)_4NPF_6$ solution (THF, N_2-degassed) on a CHI620A voltammetric analyzer with a glassy carbon working electrode ($\phi = 2$ mm), a Pt-wire auxiliary electrode and a Ag/AgCl reference electrode. The concentration of diruthenium species is always 1.0 mM. The ferrocenium–ferrocene couple was observed at 0.568 V (vs. Ag/AgCl) at the experimental conditions.

4.1. Reaction between $Ru_2(ap)_4Cl$ and large excess LiC_2Ph

To a flask containing $Ru_2(ap)_4Cl$ (0.103 g, 0.112 mmol) in 20 ml THF was added 2.24 mmol LiC_2Ph prepared in situ from HC_2Ph and ^nBuLi. The dark green solution turned to dark red immediately upon the addition of LiC_2Ph. After being stirred for 2 h under Ar, the solution was stirred in air for 30 min, during which the solution became greenish-blue. After solvent removal, the residues were loaded onto silica gel column deactivated by 10% Et_3N in hexanes and eluted with EtOAc–hexanes–Et_3N (linear gradient 0/100/5 –2/100/5, v/v). Pure compounds $Ru_2(ap)_4(C_2Ph)$ (**1a**, 0.022 g, 20% based on Ru) and $Ru_2(ap)_4(C_2Ph)_2$ (**2a**, 0.088 g, 72% based on Ru) were obtained as brown and blue crystalline materials, respectively. The former was authenticated by the FAB-mass datum. Data for **2a**, R_f, 0.72 (EtOAc –hexanes–Et_3N, 2/100/5, v/v, the same combination is also used for the determination of other R_f's); ^1H-NMR: 9.28 (q, 4H, aromatic), 7.44–7.35 (m, 8H, aromatic), 7.25–7.05(m, 7H, aromatic), 6.96–6.90

(m, 12H, aromatic), 6.32 (d, 4H, aromatic), 6.25–6.15 (m, 5H, aromatic), 5.83 (d, 6H, aromatic); ^{13}C-NMR: 105.25, 109.97; MS-FAB (*m/e*, based on ^{101}Ru): 1085 [M^+]; UV–vis, λ_{max}(nm, $\varepsilon(M^{-1}$ $cm^{-1})$), THF): 1031(3360), 629(6930), 477(5140), 430(5300); IR, ν(C≡C)/cm^{-1}, 2100.8(m), 2073.6(m); Electrochemical, $E_{1/2}$/V, ΔE_p/V, $i_{backward}/i_{forward}$: **A**, 0.723, 0.068, 0.83; **B**, −0.418, 0.059, 0.64; **C**, −1.576, 0.075, 0.38; **D**, −0.836 V.

4.2. Preparation of **2b**

Compound **1b** (0.26 g, 0.27 mmol) in 40 ml THF was treated with 8.1 mmol LiC_2Ph overnight to yield a dark red solution. Upon exposed to air, the solution gradually turned to royal blue (ca. 30 min). After the solvent removal, the residue was loaded onto silica gel column deactivated by 5% Et_3N in hexanes and eluted with EtOAc–hexanes–Et_3N (linear gradient 10/90/2 –15/85/2, v/v). Yield: 0.22 g (74% based on Ru). Data for **2b**: R_f, 0.78; ^1H-NMR: 9.15 (q, 4H, aromatic), 7.11–6.80 (m, 19H, aromatic), 6.26–6.14(m, 9H, aromatic), 5.70–5.55 (m, 9H, aromatic), 0.21 (s, 9H, Si(C$H_3)_3$); ^{13}C-NMR: 136.76, 121.43, 109.68, 104.91; MS-FAB (*m/e*, based on ^{101}Ru): 1081 [M^+]; UV–vis, λ_{max} (nm, $\varepsilon(M^{-1}$ $cm^{-1})$), THF): 1033(5130), 639(8590), 475(6260), 440(6230); IR, ν(C≡C)/cm^{-1}, 2110.0(m), 1997.3(s); Electrochemical, $E_{1/2}$/V, ΔE_p/V, $i_{backward}/i_{forward}$: **A**, 0.750, 0.069, 0.70; **B**, −0.429, 0.062, 0.90; **C**, −1.621, 0.063, 0.77; **D**, −0.843 V.

4.3. Preparation of **2c**

Same as that of **2b** except **1b** was replaced by **1c**. Yield: 65% based on Ru. Data for **2c**: R_f, 0.80; ^1H-NMR: 9.27 (q, 4H, aromatic), 7.13–6.91 (m, 17H, aromatic), 6.35–6.20(m, 10H, aromatic), 5.83–5.70 (m, 8H, aromatic), 0.32 (s, 9H, Si(C$H_3)_3$); ^{13}C-NMR($CDCl_3$): 137.01, 111.05, 109.70, 105.44, 85.51, 75.28; MS-FAB (*m/e*, based on ^{101}Ru): 1105 [M^+]; UV–vis, λ_{max} (nm, $\varepsilon(M^{-1}$ $cm^{-1})$)): 1031(4310), 640(7340), 474(5490), 439(5250); IR, ν(C≡C)/cm^{-1}, 2180.8(w), 2108.0(m), 1995.6(s); Electrochemical, $E_{1/2}$/V, ΔE_p/V, $i_{backward}/i_{forward}$: **A**, 0.804, 0.064, 0.76; **B**, −0.346, 0.062, 0.98; **C**, −1.488, 0.064, 0.97; **D**, −0.713 V.

4.4. X-ray data collection, processing, and structure analysis and refinement

Single crystals of both **2a** and **2b** were grown via slow evaporation of column chromatography fractions (hexanes–EtOAc–Et_3N). The X-ray intensity data were measured at 300 K on a Bruker SMART1000 CCD-based X-ray diffractometer system using Mo–K_α ($\lambda = 0.71073$ Å). Crystals used for X-ray crystallographic analysis were cemented onto quartz fibers with epoxy glue. Data were measured using omega scans of

Table 2
Crystal data for compounds **2a** and **2b**

	2a	2b
Empirical formula	$C_{60}H_{46}N_8Ru_2$	$C_{57}H_{50}N_8SiRu_2$
Formula weight	1081.19	1077.28
T (K)	300	300
λ (Mo–K$_\alpha$) (Å)	0.71073	0.71073
Crystal system	Triclinic	Monoclinic
Space group	$P\bar{1}$ (#2)	$C2/c$ (#15)
a (Å)	12.736(1)	14.219(2)
b (Å)	12.766(1)	25.622(3)
c (Å)	17.299(1)	13.936(2)
α (°)	70.053(1)	–
β (°)	72.738(1)	91.754(2)
γ (°)	74.365(1)	–
V (Å^3)	2480.0(2)	5074.7(9)
Z	2	4
ρ_{calc} (g cm^{-3})	1.448	1.410
μ (mm^{-1})	0.658	0.665
$F(000)$	1100	2200
Crystal size (mm)	$0.43 \times 0.18 \times 0.14$	$0.26 \times 0.12 \times 0.07$
θ range (°)	1.29–28.00	1.59–25.00
Index ranges	$-14 < h < 16$,	$-16 < h < 16$,
	$-16 < k < 16$,	$-16 < k < 30$,
	$-22 < l < 22$	$-16 < l < 16$
Reflections collected	18 797	13 271
Independent reflections	11 853	4479
	[R(int) = 0.0146]	[R(int) = 0.0435]
Refinement method	Full-matrix least-squares on F^2	Full-matrix least-squares on F^2
Data/restraints/parameters	11853/0/631	4479/6/325
Instrument	SMART1000 CCD	SMART1000 CCD
Final R indices	$R_1 = 0.029$,	$R_1 = 0.044$,
($I > 2\sigma(I)$)	$wR_2 = 0.065$	$wR_2 = 0.097$
R indices (all data)	$R_1 = 0.048$,	$R_1 = 0.079$,
	$wR_2 = 0.073$	$wR_2 = 0.112$
Goodness-of-fit on F^2	1.01	1.03
Largest difference peak and hole (e Å^{-3})	0.796 and -0.417	1.167 and -0.624

0.3° per frame such that a hemisphere (1271 frames) was collected. No decay was indicated for either data set by the recollection of the first 50 frames at the end of each data collection. The frames were integrated with the Bruker SAINT© software package using a narrow-frame integration algorithm [15], which also corrects for the Lp. Absorption corrections were applied using SADABS supplied by George Sheldrick.

The structures were solved and refined using the Bruker SHELXTL© (Version 5.1) software package [16] in the space groups $P\bar{1}$ and $C2/c$ for **2a** and **2b**, respectively. Positions of all non-hydrogen atoms of diruthenium moieties were revealed by direct method. The asymmetric unit of **2a** contains one diruthenium molecule. The asymmetric unit of **2b** contains one-half of the molecule, which is related to the other half via a crystallographic C_2 axis passing through Ru–Ru bond. With all non-hydrogen atoms being anisotropic and all

hydrogen atoms in calculated position and riding mode the structure was refined to convergence by least squares method on F^2 (SHELXL-93, incorporated in SHELXTL.PC V 5.03) [17,18]. Relevant information on the data collection and the figures of merit of final refinement is given in Table 2.

5. Supplementary material

Crystallographic data for the structural analysis have been deposited with the Cambridge Crystallographic Data Center, CCDC nos. 181524 and 181523 for compounds **2a** and **2b**, respectively. Copies of this information may be obtained free of charge from The Director, CCDC, 12 Union Road, Cambridge CB2 1EZ, UK (Fax: +44-1223-336033; e-mail: deposit@ccdc.cam.ac.uk or www: http://www.ccdc.cam.ac.uk)

Acknowledgements

References

[1] A.R. Chakravarty, F.A. Cotton, Inorg. Chim. Acta 113 (1986) 19.
[2] J.L. Bear, B. Han, S. Huang, J. Am. Chem. Soc. 115 (1993) 1175.
[3] J.L. Bear, B. Han, S. Huang, K.M. Kadish, Inorg. Chem. 35 (1996) 3012.
[4] J.L. Bear, Y. Li, B. Han, E.V. Caemelbecke, K.M. Kadish, Inorg. Chem. 36 (1997) 5449.
[5] C. Lin, T. Ren, E.J. Valente, J.D. Zubkowski, J. Chem. Soc. Dalton Trans. (1998) 571.
[6] C. Lin, T. Ren, E.J. Valente, J.D. Zubkowski, J. Organomet. Chem. 579 (1999) 114.
[7] G. Zou, J.C. Alvarez, T. Ren, J. Organomet. Chem. 596 (2000) 152.
[8] T. Ren, G. Zou, J. Alvarez, Chem. Commun. (2000) 1197.
[9] G. Xu, T. Ren, Organometallics 20 (2001) 2400.
[10] G. Xu, T. Ren, Inorg. Chem. 40 (2001) 2925.
[11] T. Ren, Organometallics 21 (2002) 732.
[12] G. Xu, T. Ren, Inorg. Chem. 41 (2002) in press.
[13] T. Ren, Coord. Chem. Rev. 175 (1998) 43.
[14] P. Siemsen, R.C. Livingston, F. Diederich, Angew. Chem. Int. Ed. Engl. 39 (2000) 2632.
[15] SAINT V 6.035 Software for the CCD Detector System, Bruker-AXS Inc., 1999.
[16] SHELXTL-5.03 (WINDOW-NT Version), Program library for structure solution and molecular graphics, Bruker-AXS Inc., 1998.
[17] G.M. Sheldrick, SHELXS-90, Program for the Solution of Crystal Structures, University of Göttigen, Germany, 1990.
[18] G.M. Sheldrick, SHELXL-93, Program for the refinement of crystal structures, University of Göttigen, Germany, 1993.